Environmental Microbiology (2018) **20**(12), 4486–4502 doi:10.1111/1462-2920.14385

Metabolic specialization of denitrifiers in permeable sediments controls N_2O emissions

Hannah K. Marchant,[1*] **Halina E. Tegetmeyer**,[1,2] **Soeren Ahmerkamp**,[1] **Moritz Holtappels**,[1†] **Gaute Lavik**,[1] **Jon Graf**,[1] **Frank Schreiber**,[1,3,4,5] **Marc Mussmann**,[1‡] **Marc Strous**[1§] **and Marcel M. M. Kuypers**[1]

[1]*Max Planck Institute for Marine Microbiology, Bremen, Germany.*

[2]*Center for Biotechnology, Bielefeld University, Bielefeld, Germany.*

[3]*ETH Zurich, Swiss Federal Institute of Technology, Department of Environmental Systems Science, Zurich, Switzerland.*

[4]*Eawag, Swiss Federal Institute of Aquatic Science and Technology, Department of Environmental Microbiology, Dübendorf, Switzerland.*

[5]*Division of Biodeterioration and Reference Organisms, Department of Materials and Environment, Federal Institute for Materials Research and Testing (BAM), Berlin, Germany.*

Summary

Coastal oceans receive large amounts of anthropogenic fixed nitrogen (N), most of which is denitrified in the sediment before reaching the open ocean. Sandy sediments, which are common in coastal regions, seem to play an important role in catalysing this N-loss. Permeable sediments are characterized by advective porewater transport, which supplies high fluxes of organic matter into the sediment, but also leads to fluctuations in oxygen and nitrate concentrations. Little is known about how the denitrifying communities in these sediments are adapted to such fluctuations. Our combined results indicate that denitrification in eutrophied sandy sediments from the world's largest tidal flat system, the Wadden Sea, is carried out by different groups of microorganisms. This segregation leads to the formation of N_2O which is advectively transported to the overlying waters and thereby emitted to the atmosphere. At the same time, the production of N_2O within the sediment supports a subset of *Flavobacteriia* which appear to be specialized on N_2O reduction. If the mechanisms shown here are active in other coastal zones, then denitrification in eutrophied sandy sediments may substantially contribute to current marine N_2O emissions.

Received 17 October, 2016; revised 10 August, 2018; accepted 12 August, 2018. *For correspondence. E-mail hmarchan@mpi-bremen.de; Tel.: +49 04212028630. †Present address: Alfred Wegener Institute, Helmholtz Center for Polar and Marine Research, Bremerhaven
‡Present address: Division of Microbial Ecology, Vienna
§Present address: University of Calgary, Calgary, Alberta, Canada

Introduction

The continental shelves and specifically coastal regions act as a buffer between the land and open ocean, making them vulnerable to anthropogenically induced eutrophication. In these regions, sands cover more than 50% of the seafloor (Emery 1968, Hall 2002), however little is known about the role of sandy sediments in global biogeochemical cycles of carbon and nitrogen. Since the 1860's nitrogen (N) inputs to coastal regions from riverine and land drainage have more than doubled, while atmospheric N-deposition has risen sixfold, leading to current day inputs of around 90 Tg N yr^{-1} (Dentener *et al*. 2006, Gruber and Galloway 2008). In the world's largest intertidal area, the Wadden Sea, which is predominantly comprised of sandy sediments, nitrate inputs have increased eightfold since the 1930's (van Beusekom 2005).

The advection of seawater into permeable sands creates porewater flow, filtering out organic matter and delivering nutrients and electron acceptors (e.g. oxygen and nitrate) at rates orders of magnitude higher than diffusive fluxes (Huettel *et al*., 2003). However the redox conditions in permeable sands are highly variable over time scales of minutes to hours (Huettel *et al*., 2014, Jansen et al, 2009). This is a result of changes in the magnitude of porewater flow, which is controlled by bottom water currents, sediment topography and sediment transport (Ahmerkamp *et al*., 2015, Ahmerkamp *et al.,* 2017). The combination of high fluxes with microbial abundances of around 10^9 cells ml^{-1} sediment (Musat *et al*., 2006), means that permeable sediments act as biocatalysts, enhancing oxygen respiration and denitrification rates (Gao *et al*. 2012, Janssen *et al*. 2005, Marchant *et al*. 2016, Sokoll *et al*. 2016). Consequently, large amounts of anthropogenic N-inputs that enter coastal regions can

be removed within permeable sediments. Still, little is known about how the microbial communities mediating denitrification in permeable sediments cope with the large fluctuations in oxygen and substrate availability that occur on small spatial and temporal scales.

Denitrification is a four-step, modular process, carried out by microorganisms with highly branched respiratory chains. Almost all steps can be catalysed by more than one enzyme, therefore the complete reduction of NO_3^- to N_2 can occur via at least 12 different routes (Schreiber *et al*., 2012, Simon and Klotz 2013, Kuypers *et al.,* 2018) with each enzyme differing in its affinity, reaction rate and response to environmental factors (Philippot and Hallin 2005). Furthermore, each intermediate reaction of the denitrification pathway can occur independently from the others. While denitrification is often studied in model organisms that are 'complete' denitrifiers, it is becoming apparent that a network of N-cycling microorganisms might be responsible for environmental denitrification, with diverse microbes specialized to respire only one or some of the intermediates (Graf *et al*., 2014, Kuypers *et al*., 2018, Lilja and Johnson 2016, Philippot *et al.,* 2013, Roco *et al.,* 2016).

It has been recognized for many years that some denitrifiers lack a nitrous oxide (N_2O) reductase (Henry *et al*. 2006, Jones *et al*. 2008, Wood *et al*. 2001). Therefore in these organisms denitrification is truncated and produces N_2O, a potent greenhouse gas that is also the most important present day contributor to ozone-depletion (Ravishankara *et al*. 2009). The presence of truncated denitrifiers has been assumed to play a large role in determining N_2O emissions. Other factors that are implicated in controlling N_2O emissions include imbalances in the coupling of individual denitrification steps within single organisms, and the functioning of N_2O reductase itself (Dendooven and Anderson 1994, Naqvi *et al*., 2000, Seitzinger *et al*. 1983, Šimek and Cooper 2002).

Recently, sequencing studies have identified a subset of denitrifiers which only possess N_2O reductase (Sanford *et al*., 2012) and there is growing evidence that these organisms have a strong influence on the amount of N_2O released from terrestrial soils (Graf *et al*. 2014, Hallin et al., 2018, Jones *et al*. 2012, Jones *et al*. 2014). Theoretically, N_2O reduction is one of the most thermodynamically favourable steps of the denitrification pathway, with a $\Delta G'^0$ of −677 kJ/mol CH_2O compared to −352 kJ/mol CH_2O for nitrate reduction to nitrite or − 464 kJ/mol CH_2O for nitrite reduction to N_2O (in typical marine sediment conditions of 10 μM NO_3^-, 1 μM NO_2^-, 7.2 nM N_2O, 10 μM CH_2O, pH 8.2, salinity 35 PSU). So far however, little is known about the abundance or ecological role of N_2O reducers, especially in shallow coastal marine sediments where N_2O dynamics are poorly constrained. Despite the fact that on average 0.01 mol of N_2O is produced for every mol of N_2 released from marine sediments (Seitzinger *et al*., 2000, Usui *et al.,* 2001), fluxes of N_2O out of shallow coastal sediments vary widely, and in some cases are even negative (Foster and Fulweiler 2016, Murray *et al.,* 2015, Schutte *et al.,* 2015). Most previous studies on benthic marine N_2O emissions have focused on cohesive sediments where N_2O is largely consumed as it diffuses out of the sediment (Meyer *et al.,* 2008). In the few cases where sandy sediments have been investigated the effect of enhanced transport due to porewater advection has been neglected, although this might lead to greater N_2O fluxes to the water column.

Permeable sandy sediments have high N-loss potentials compared to other marine environments and therefore any imbalances in N_2O production and N_2O consumption resulting from community specialization and rapidly fluctuating conditions could have a significant impact on marine N_2O budgets. Our aim in this study was to investigate the influence of such rapid fluctuations on the occurrence of truncated forms of denitrification and the associated production and consumption of N-oxides. In order to investigate this we sampled at a sand flat in the Wadden Sea, where denitrification removes up to 60% of riverine N inputs (Gao *et al.,* 2012) and the dynamic conditions are representative of coastal permeable sediments. We repeated measurements in different months to ensure the consistency of results, however, we did not sample regularly throughout the year as the current study did not aim to make yearly or seasonal budgets for the sand-flat. Incubations in flow through sediment cores were carried out to examine the production and consumption patterns of denitrification intermediates (NO_2^-, N_2O). These experiments were repeated under both dynamic and steady state conditions to study how oxygen concentrations influenced denitrification dynamics. Furthermore, we investigated how advection transports N_2O to the water column, both in laboratory incubations and *in situ.* To gain insights into whether community structure has an effect on the net production of denitrification intermediates, experimental work was combined with *in situ* data on the occurrence of functional denitrification genes within the sediment and their transcription over a tidal cycle.

Results

Nitrification

To investigate potential nitrification rates and N_2O production associated with nitrification, sediments were incubated with oxic water amended with $^{15}NH_4^+$ and $^{14}NO_2^-$. Ammonia oxidation was always detected, although rates (0.22 ± 0.02 mmol N $m^{-3}_{sediment}$ h^{-1}) were low compared to denitrification (see below) throughout the year. N_2O formation after addition of $^{15}NH_4^+$ and $^{14}NO_2^-$ was always below detection limit, indicating that nitrification

does not contribute significantly to N_2O production in these sediments.

Denitrification under steady state anoxic conditions

Denitrification and the presence of denitrification intermediates in the porewater of sediment (i.e. NO_2^-, N_2O and N_2) were investigated under steady state anoxic conditions in sediment collected in August 2015 in three replicate flow through columns. Each column was supplied with anoxic water containing 60 μmol L^{-1} $^{15}NO_3^-$. In total 53.5 μmol L^{-1} of $^{15}NO_3^-$ was consumed within the sediment, resulting in outlet concentrations of 6.5 μmol NO_3^- L^{-1}. $^{15}NO_2^-$ concentrations rose from undetectable at the inlet to 22 ± 1.2 NO_2^- μmol L^{-1} at the core outlet, while 0.112 ± 0.02 μmol L^{-1} $^{15N\text{-}N}{}_2O$ and 7.8 ± 0.7 μmol L^{-1} $^{15}N{-}N_2$ were measured at the core outlet. Therefore 60% of the added $^{15}NO_3^-$ was accounted for, the other 40% most likely entered intracellular pools or was converted to $^{15}NH_4^+$ by organisms carrying out DNRA (see Marchant *et al*., 2014).

Denitrification under changing conditions

Rates of denitrification and the production and consumption rates of denitrification intermediates (NO_2^- and N_2O) were measured in cores in which incubations were started under oxic conditions and amended with varying amounts of $^{15}NO_3^-$. Three replicate cores were filled with sediment and repeatedly amended with $^{15}NO_3^-$ at different concentrations. During each amendment time series of up to 30 data points were collected.

When cores were amended with only 15 μmol L^{-1} $^{15}NO_3^-$, consumption of NO_3^- began immediately (while the sediment was still oxic) and NO_3^- was entirely consumed within 40 min (Fig. 1A). N_2 was produced from the start of the incubation. Net NO_2^- production occurred for around 20 min and net consumption began when both O_2 and NO_3^- concentrations dropped below 10 μmol L^{-1}. Net N_2O production was observed for the first 20 min, then concentrations stayed stable and net N_2O consumption occurred when NO_3^- and NO_2^- were depleted. When cores were amended with 50 μmol L^{-1} $^{15}NO_3^-$, similar patterns were observed as the 15 μmol L^{-1} incubations, i.e. net N_2O production occurred at the start of the incubation and N_2O concentrations stabilized as NO_3^- and NO_2^- dropped. Net N_2O consumption only occurred after NO_2^- production had ceased (Fig. 1B).

When the cores were amended with 100 μmol L^{-1} $^{15}NO_3^-$, NO_3^- was not entirely consumed by the end of the incubation. A small net production of NO_2^- was observed initially followed by net consumption of NO_2^-. Net production of N_2O and N_2 was observed throughout the incubation (Fig. 1C). When the cores were amended with 500 μmol L^{-1} NO_3^-, the NO_3^- was not entirely consumed by the end of the incubation. Net production of NO_2^-, N_2O and N_2 was observed throughout the incubation (data not shown).

In all three sediment cores, regardless of starting $^{15}NO_3^-$ concentration N_2O and N_2 were produced under oxic conditions; N_2 and N_2O production rates were calculated from time points when O_2 was still present in the porewater and from time points after O_2 had been consumed. N_2 production rates were substantially lower in the oxic phase than in the anoxic phase (1.26 ± 0.43 mmol N m^{-3} h^{-1} and 3.45 ± 1.2 mmol N m^{-3} h^{-1} respectively), however N_2O production rates did not differ significantly between oxic (0.060 ± 0.024 mmol N m^{-3} h^{-1}) and anoxic conditions (0.053 ± 0.023 mmol N m^{-3} h^{-1}) (student *t*-test, p = >0.05, df = 16). The ratio of N_2O:N_2 production was therefore higher in the presence of O_2 than in its absence (oxic = 4.5% and anoxic = 1.6%, student *t*-test $p < 0.01$).

In three other seasons, the ratio of N_2O:N_2 under oxic and anoxic conditions was determined in triplicate sediment cores during time series incubations (rates of N_2 production and DNRA for the same incubations are presented in Marchant *et al*., 2014). Similar ratios were observed in all seasons (N_2O:N_2 Oxic = 4.3 ± 1.4, 2.1 ± 0.3, 3.1 ± 1.7 and anoxic = 0.7 ± 0.06, 0.5 ± 0.3, 1.2 ± 0.5 SD, in November, April and July respectively).

Transport of N_2O from the sediment to the water column

To investigate whether advection and the resulting enhancement of porewater transport leads to N_2O emissions from the sediment, water was pumped from the bottom of a sediment core at velocities comparable to those measured in similar sediments *in situ* (11 and 21 cm h^{-1} (Billerbeck *et al*. 2006b, Precht and Huettel 2004)). Over time, transport of aerated, NO_3^- amended seawater through the column increased the oxygen concentration within the upper layers of the sediment column, and also led to rises in the N_2O concentration within the sediment (Fig. S6). The N_2O formed within the sediment was subsequently transported to the water overlying the sediment (Fig. 2). The flux of N_2O to the overlying water increased with increasing flow velocity.

To investigate whether similar transport of N_2O from the sediment to the water column is observed *in situ* we measured water column NO_x (nitrate and nitrite) and N_2O concentrations directly above an intertidal permeable sand flat in the Wadden Sea in May 2011. Water column N_2O was on average 156% ± 3.9 *SD* (n = 34) over-saturated and neither NO_x nor N_2O varied significantly with depth or tidal duration. Based on the water column concentration of N_2O, sea-air fluxes between 1.10 and 1.50 μmol m^{-2} h^{-1} were calculated using two different parameterizations of air-sea gas exchange. As such daily export of N_2O from the back barrier region to the German Bight would be

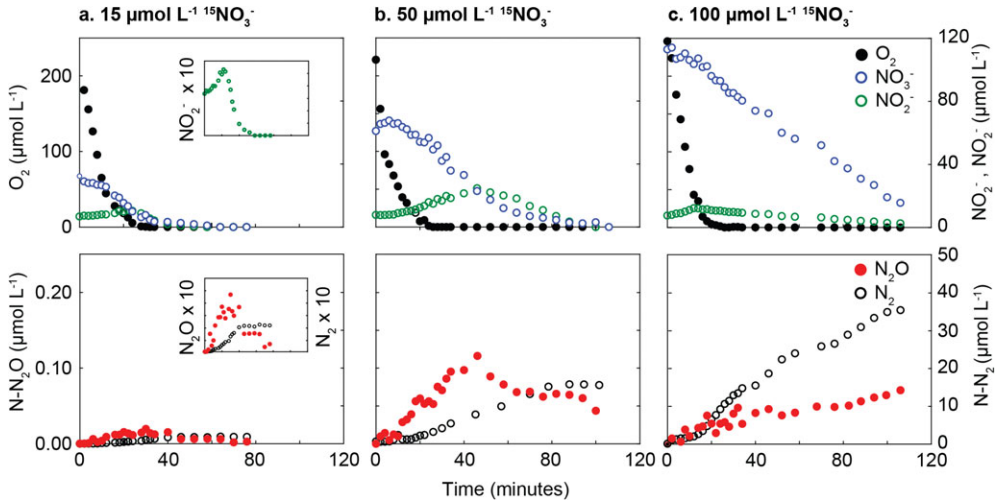

Fig. 1. The production and consumption of denitrification intermediates during dynamic incubations. Sediment columns were percolated with aerated seawater spiked with different starting concentrations of $^{15}NO_3^-$ and the production and consumption of denitrification intermediates was determined over time both while O_2 was still present and after the columns became anoxic. N—N_2 and N—N_2O concentrations are the total production of N as either N_2 or N_2O determined from the measured $^{29}N_2$ and $^{30}N_2$ or $^{45}N_2O$ and $^{46}N_2O$ concentrations. The inlays show the NO_2^-, N—N_2O and N—N_2 concentrations magnified 10× in comparison to the y-axis on the main plots (the x-axis remains 0–120 min).

84 mol day^{-1}, whereas daily air-sea exchange for the same area was in the range of 1162–2302 mol day^{-1}. To confirm that the source of N_2O was within Wadden Sea sediments, we measured N_2O concentrations at a tidal inlet, where water from the North Sea enters the back-barrier Wadden Sea region as the tide rises. Strong tidal variations in N_2O over-saturation were observed at the tidal inlet (Fig. 2); water entering from the North Sea at high tide was around 3% over-saturated. At low tide, the N_2O over-saturation of water leaving the back barrier region was around 10 times higher (~ 27% over-saturated).

Based on a transport model, the experimentally determined volumetric N_2O and N_2 production rates were used to calculate areal fluxes of N_2O and N_2 out of the sediment (Table 1). The sediment was always a source of N_2O to the water column.

Sediment community

Phylogeny. To investigate the sediment microbial community we analysed the taxonomic distribution of all sequences in the 454 metagenomic datasets. Our results indicated that the microbial community in October and March were similar, i.e. the percentage of sequences assigned to each class all fell within 1.5 standard deviations of the mean (Supporting Information Table S2), with one exception - the Bacillariophyta were most dominant in March, but less so in October. The Bacteroidetes and Proteobacteria were the two dominant microbial phyla present within the sediment (Supporting Information Table S2). Within the Bacteriodetes, the class *Flavobacteriia* was the most abundant. Within the Proteobacteria, *Gammaproteobacteria* were most abundant, followed by *Alphaproteobacteria, Betaproteobacteria* and the Delta/Epsilon divisions.

Taxonomic distribution of denitrification functional genes. Functional genes for all steps of the denitrification pathway (*napA*, *narG, nirS, nirK, norB,* and *nosZ*) were detected in similar proportions in the 454 metagenomes [independent of detection approach (HMM or ROCker)] and the Illumina metagenome (Fig. 3).

Phylogenetic assignments of functional denitrification genes in the 454 datasets determined using both MEGAN and Kaiju were similar at both the phyla and class level (Supporting Information Fig. S1). Relative abundance and phylogenetic assignment of all reads using ROCker and Kaiju are shown in Fig. 3. The genes for nitrate, nitrite and nitric oxide reduction (*napA*, *nirS*, *norB*) were found to be most similar to known gammaproteobacterial genes. For *narG*, most reads were associated to the *Gammaproteobacteria, Deltaproteobacteria* and *Alphaproteobacteria.* When analysing all functional denitrification genes assigned to the *Gammaproteobacteria*, the distribution of genes between each step of the pathway was relatively even (Supporting Information Table S3), independent of sequencing technology, detection method and assignment method.

In comparison, the detected genes for nitrous oxide reductase (*nosZ*) were most similar to genes of the Bacteroidetes, in particular, the *Flavobacteriia* (139 of 247 total nosZ counts in the 454 metagenome and 4928 of 13471 in the Illumina metagenome). In the 454 data the average odds ratio (the number of *Flavobacteriia nosZ* reads divided by the number of all other *Flavobacteriia* denitrification reads over the number of gammaproteobacterial *nosZ* reads divided by the number of all other *Gammaproteobacteria* denitrification reads) of all four metagenomes for *Flavobacteriia* was 7.1 ± 1.2 when based on both total read numbers and 6.9 ± 1.0 based on coverage per base. For the Illumina dataset the odds ratio was 26 based on total read numbers and 39 based on coverage per base. Values substantially

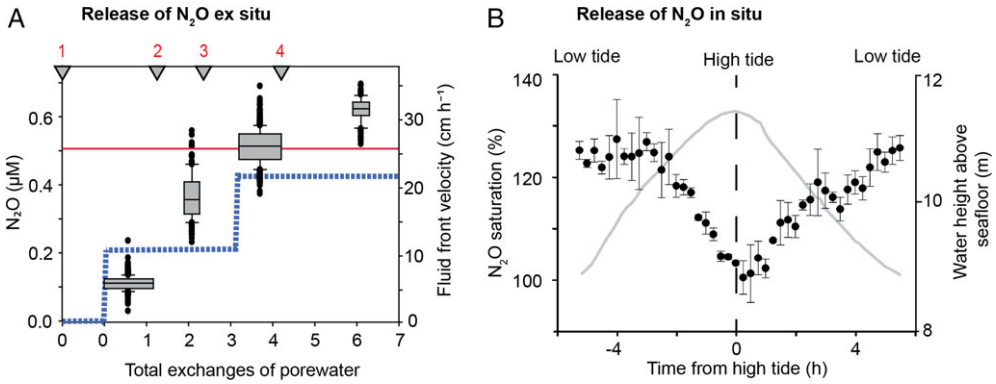

Fig. 2. Release of N_2O to the water column through advection. A. N_2O concentrations (box plots) in the water column above a sediment column though which aerated seawater was supplied from the bottom at realistic flow velocities (blue dashed line, red line represents in situ flow velocity measured previously in similar sediment). Triangles and associated numbers represent the start of sediment profiles which took 45 min to complete (Supporting Information Fig. S5). B. Tidal changes in N_2O saturation of surface waters at a tidal inlet to the Wadden Sea. The tidal prism is represented by the grey line. Vertical bars represent *SD* (n = 3).

greater than one in odds ratio analysis indicate that the ratio of *nosZ* to other denitrifying genes was much higher in the *Flavobacteriia* than for the *Gammaproteobacteria.*

Transcription of functional genes across a tidal cycle. Metatranscriptomes were sampled directly from the sand flat at six time points over a tidal cycle. Transcripts were identified for each of the denitrification marker genes in all metatranscriptomes (Fig. 4*, narG, napA, nirK, nirS, norB, nosZ*). *napA* had the highest relative abundance (when read counts were normalized to gene length and total number of mRNA reads in the metatranscriptome), followed by *narG* and *norB.* Counts of *nirK, nirS* and *nosZ* were lower (Supporting Information Fig. S3).

Transcripts that were phylogenetically affiliated to the *Gammaproteobacteria* dominated the relative counts of *napA* (89 ± 3%), *narG* (80 ± 7%) and *norB* (74 ± 12%) at all time points. Reads for *nirS* and *nirK* were more homogenously distributed across groups, while reads affiliated to the Bacteroidetes, specifically the *Flavobacteriia*, dominated the *nosZ* transcripts [on average 44 ± 12% of *nosZ* transcripts were associated to the *Flavobacteriia*, the highest percentage was observed at late low tide (59%)].

Taxonomic distribution of Flavobacteriia *denitrification genes and transcripts.* Of the total 247 validated *nosZ* encoding metagenomic reads, all could be aligned via blastx to a reference sequence with an e-value of < e^{-6}. For 184 reads the e-value was ≤ e^{-30}, for 104 reads the e-values were < e^{-49}, and for 16 reads the e-values were < e^{-100}. All sequences had a top five blastp hit to an annotated *nosZ* sequence. BLAST analysis followed by assignment using MEGAN or Kaiju revealed that the majority of the *Flavobacteriia nosZ* reads were related to members of the Flavobacteriaceae. While assignments were more variable at genus level, generally the most common assignments were to the genera *Muricauda* and *Eudoraea* (Supporting Information Fig. S2).

Within the metatranscriptomes, transcripts taxonomically assigned to *Flavobacteriia* were found within the *napA*, *narG, nirK, norB* and *nosZ* reads. However, at all time points, the transcripts taxonomically assigned to the *Flavobacteriia* were mainly *nosZ* rather than other denitrification pathway genes (Fig. 4 and Supporting Information Fig. S4). Of the sequences which could be taxonomically assigned to genera level, most were assigned as either *Muricauda* or *Eudoraea* (Supporting Information Fig. S5). Of the 425 *Flavobacteriia nosZ* transcripts (all of which had an e-value < e^{-7}), 124 had a top blastp hit to *Eudoraea adriatica* and 24 to *Muricauda sp. MAR_2010_75.* In contrast, no *napA, narG, nirS* or *norB* transcripts were assigned to the *Muricauda* or *Eudoraea* genera.

Discussion

Production and consumption of denitrification intermediates indicates metabolic specialization by denitrifiers

Intertidal sandy sediments are highly dynamic environments, where oxygen and nitrate availability differ on cm to mm scales and between high tide and low tide.

Table 1. Benthic fluxes of O_2, N_2O and N_2 in March 2011 derived from combining volumetric rates obtained in $^{15}NO_3^-$ stable isotope labeling experiments with a transport model for permeable sediments. The bottom water velocities are representative of different current speeds during a tidal cycle at the sand flat.

Bottom water velocity cm s^{-1}		O_2 flux µmol O_2 m^2 h^{-1}	N_2O flux µmol N m^2 h^{-1}	N_2 flux	% N-loss as N_2O
Minimum	7.6	–437	0.11	17.1	0.7
Average	25	–3523	0.93	63.9	1.4
Maximum	42	–6957	1.51	85.2	1.5

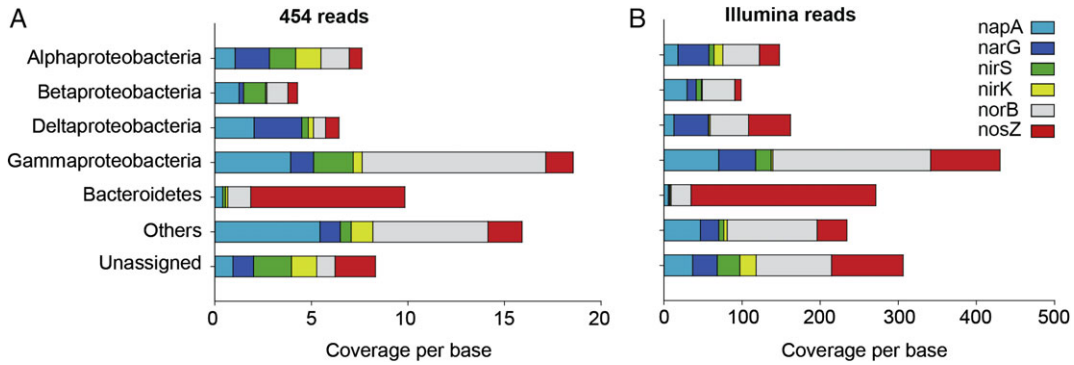

Fig. 3. Phylogenetic affiliation of functional gene reads in all metagenomes. A. Compiled data from one sample in October 2009 and two samples in March 2010 sequenced with 454 GS FLX titanium. B. Data from one sample in April 2013 sequenced with a HiSeq2000 Illumina platform. Reads were identified using ROCker and taxonomically assigned using Kaiju. See Supporting Information Fig. S1 for a comparison to an HMM-based approach and taxonomic assignment using MEGAN. Coverage per base refers to the sum of all read bases aligning to a functional gene, divided by the average length of that gene.

Furthermore, redistribution of sand means that microbes attached to sand grains can move rapidly between conditions. Here we used a number of experimental approaches on bulk sediments which integrate the small scale variability observed in these sediments and allow the study of biogeochemical processes.

High rates of denitrification in the presence and absence of oxygen have been observed before in the permeable sediments of the Wadden Sea (Gao *et al*., 2010, Gao *et al*. 2012, Marchant *et al*. 2014). So far however, little is known about the balance between consumption and production of denitrification intermediates in this dynamic intertidal environment. In this study we could confirm that denitrification rates within intertidal sandy sediments from the Wadden Sea were high and were associated with the accumulation of NO_2^- and N_2O. Nitrification rates were always at least an order of magnitude lower than denitrification, independent of season, and were not associated with detectable N_2O accumulation.

When the sediment was kept anoxic and supplied continuously with replete nitrate, there was a net production of the denitrification pathway intermediates NO_2^- and N_2O, with net production rates around 380% and 1.4%, respectively, of the N_2 production rate. Such accumulation of denitrification intermediates may have resulted from two factors; 1) poor coupling of individual denitrification steps within single organisms (Bergaust *et al*., 2008, Lilja and Johnson 2016, Otte *et al*. 1996, Philippot *et al*. 2001) or; 2) process partitioning within the denitrifying community, i.e. the presence of truncated forms of

Fig. 4. Uneven taxonomic distribution of denitrification functional gene transcripts across a tidal cycle.

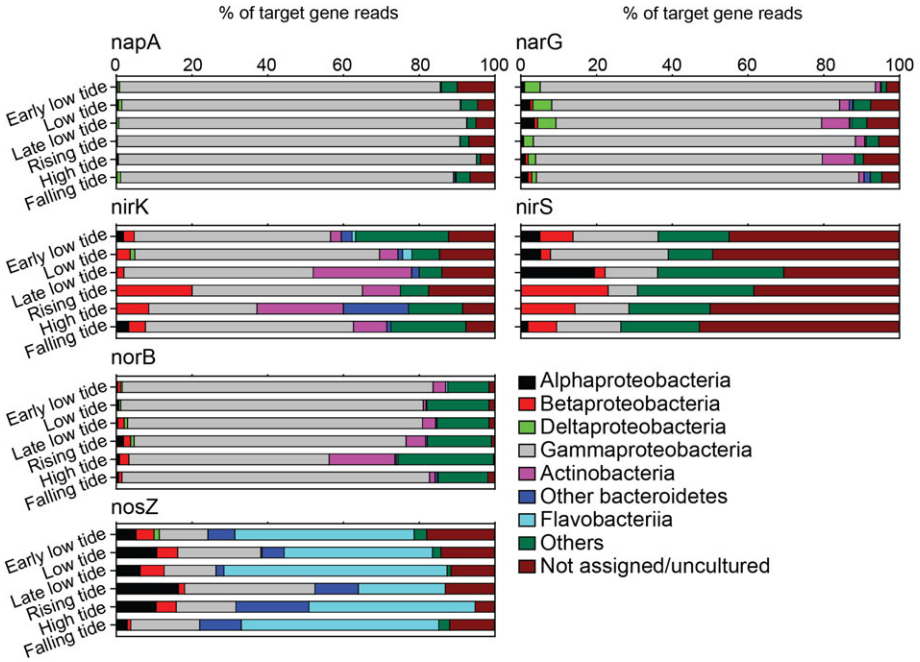

denitrification in different community members (Graf *et al*. 2014, Kuypers *et al*. 2018, Roco *et al*. 2016, Shapleigh 2007). The particularly large accumulation of nitrite provided a first indication that nitrate reduction might be mediated by different members of the community than the rest of the pathway in sandy sediments, similar to other environments where nitrate reduction rates are orders of magnitude higher than N_2 production rates (Ganesh *et al*. 2015, Kalvelage *et al*. 2013). Still, steady state conditions provide little insight into these factors as they reduce complex environmental conditions to their most simple form (i.e. constant anoxia or replete nitrate availability). Therefore, we investigated the causes of net NO_2^- and N_2O production in more detail.

To imitate the fluctuations of oxygen and nitrate that occur *in situ* (Ahmerkamp *et al.,* 2015, Billerbeck *et al.,* 2006b, Marchant et al, 2017) we investigated the appearance and disappearance of denitrification products in the porewater (NO_2^-, N_2O and N_2) under dynamic conditions. Incubations were started under oxic conditions, with initial $^{15}NO_3^-$ concentrations ranging from 15 to 500 μmol L^{-1} (Fig. 1) and over time oxygen and NO_3^- were consumed. Denitrification occurred in the presence of oxygen, but at a lower rate compared to anoxic conditions. However, there was a significantly higher ratio of N_2O : N_2 production in comparison to anoxic conditions. This pattern of N_2O : N_2 production was observed in triplicate sediment cores across different seasons, despite large variations in denitrification rates. Enhanced N_2O production in the presence of oxygen can be attributed to the inefficient coupling of denitrification enzymes, due to the partial deactivation of nitrous oxide reductase by oxygen (Dendooven and Anderson 1994), or from mismatches in the expression of nitrous oxide reductase relative to nitrate and nitrite reductases (Bakken *et al*. 2012). We hypothesise that the lower N_2O : N_2 ratio under anoxic conditions may also have been due to higher activity of specialized N_2O reducers. Evidence for this is provided by both the changes in intermediate N-oxide production in the transient incubations and by the distribution of functional genes observed in the molecular data (see below).

When the sediment became anoxic, N_2 production rates rose and there was a net consumption of NO_2^- and N_2O when NO_3^- and subsequently NO_2^- became limiting within the porewater (Fig. 1). In the incubations to which 500 μmol L^{-1} $^{15}NO_3^-$ were added and NO_3^- was never fully depleted, both NO_2^- and N_2O continued to accumulate steadily even as N_2 was produced. These results indicate truncated forms of denitrification occur within the sediment, where nitrate reduction to nitrite and incomplete denitrification by some community members results in net NO_2^- and N_2O production in the presence of nitrate. There is then a net consumption of N_2O when nitrate and nitrite become limiting by specialized N_2O reducers.

Metagenomic and metatranscriptomic evidence for metabolic specialization within the denitrifying community

The incidence of truncated forms of the denitrification pathway in a large proportion of the denitrification community is supported by the uneven taxonomic distribution of denitrification genes within the sediment (Fig. 3). The same patterns were detected independent of sequencing technology or analysis pipeline. Furthermore, the distribution of denitrifying genes was remarkably consistent regardless of the sampling time point (October 2009, March 2010 and April 2013), although we cannot exclude that the community differed during other seasons. For example, there was a higher read abundance and higher coverage of genes from the first three steps of the denitrification pathway (*napA, narG, nirK* and *norB*) in gammaproteobacterial groups. Similarly, reads matching the nitrate reductases (*narG* and *napA*) and nitric oxide reductase were more common in the *Deltaproteobacteria* than those for nitrite and nitrous oxide reductase. This suggests that within these two groups, many organisms might carry out only nitrate reduction to nitrite, or truncate their denitrification pathway before the nitrous oxide reduction step.

Recently, metagenomic evidence from uncultured *Gammaproteobacteria* (*Woeseiaceae*/JTB255-MBG) abundant at the sampling site and in other sediments worldwide has suggested that these organisms only have a truncated denitrification pathway (i.e. they can only reduce NO_2^- to N_2O) (Mussmann *et al*., 2017). The short read length of our sequences and the poor representation of *nirS* from cultured representatives in the databases makes it difficult to assign our sequences to a phylogenetic level beyond class. However, of the sequences that were recovered, 52% of the validated *nirS* reads in the 454 metagenomes had a blast hit similar (up to 90%) to *Woeseiaceae*/JTB255-MBG *nirS* sequences. Furthermore, the *Woeseiaceae*/JTB255-MBG *nirS* sequences clustered with many of the uncultured bacteria sequences which were the closest blast hits of the validated *nirS* sequences (Supporting Information Fig. S7). Future investigations will provide insights into the importance of this organism for denitrification within permeable sediments.

Even more strikingly, more than half of the nitrous oxide reductases were assigned taxonomically to the *Flavobacteriia.* Moreover, more than 95% of the denitrification pathway genes assigned to the *Flavobacteriia* encoded nitrous oxide reductases. We analysed the phylogenetic affiliations of the 92 *Flavobacteriia nosZ* sequences detected in our 454 metagenomes more

closely (Supporting Information Figs. S5 and S8). This revealed that the majority of *Flavobacteriia nosZ* genes were similar to homologous genes of either *Muricauda sp. MAR_2010_75*, or *Eudoraea adriatica* (DSM 19308). No other functional genes of the dissimilatory denitrification pathway were found for these organisms in the metagenomes or for any other organism in the same genera. There is a possibility that the *Flavobacteriia* within the sediment have obtained other N-oxide reductases via lateral gene transfer, making a simple assignment unreliable. However, the complete genomes which are available for *Muricauda sp. MAR_2010_75* and *Eudoraea adriatica* also only encode nitrous oxide reductase and no other denitrification pathway genes. We confirmed that no further denitrification genes were present in these genomes during our own reanalysis (data not shown). Combined with the relatively high coverage of *Flavobacteriia* sequences in the metagenomes (Supporting Information Table S2), a more likely explanation for the overabundance of *Flavobacteriia* N_2O reductases is that the *Flavobacteriia* present in the sediment only encoded nitrous oxide reductase.

The metatranscriptomic data also supports metabolic specialization by denitrifiers within the sediment. Few trends could be seen across the tidal cycle when the different genes were examined individually (Fig. 4 and see Marchant *et al*., 2017). This suggests that there is no strong response at the transcriptional level to the large fluctuations that occur over a day at the sand flat. What was highly apparent was that nitrate and nitric oxide reductases were more highly transcribed than the nitrite and nitrous oxide reductases (Supporting Information Fig. S3). While transcription does not equate to activity and it seems likely that we could not identify all nitrite reductase transcripts, the general trends in the transcriptomic data agree with the rate-based evidence that there are imbalances in the production and consumption of denitrification intermediates. Furthermore, the taxonomic assignment of nitrous oxide reductase transcripts matched those of the metagenomes (Supporting Information Figs. S2 and S3), i.e. more than half of the *nosZ* transcripts were assigned to the *Flavobacteriia*, specifically to the same two genera that were abundant in the metagenomes. Of these, we could find no other denitrification pathway gene transcripts affiliated to genera *Eudoraea* or *Muricauda.* Taking into account all of the *Flavobacteriia* denitrification transcripts, *nosZ* reads were always the most transcribed gene at all points across the tidal cycle (Fig. 4 and Supporting Information Fig. S4). Together the metagenonomic and metatranscriptomic data suggest that at the times we sampled, imbalances in the production and consumption of denitrification intermediates are driven largely by community composition and the suite of denitrifying genes that microorganisms encode. Changes in transcription in response to fluctuations in the sand flat seemed to play a more minor role.

Members of the *Flavobacteriia* are ubiquitous and abundant in the sandy sediments that fringe North-West Europe. Fluorescence *in situ* hybridization counts made along a 2000 km stretch of the coastline have shown that between 7% and 20% of the sediment community belong to the *Flavobacteriia* (Rizvi 2014). At the same time, between 5% and 8% of 16S amplicon sequences derived from the upper layers of the sediment in the Wadden Sea are assigned to *Flavobacteriia* of which the genus *Eudoraea* were the most abundant single group (Dyksma *et al.,* 2016). Similarly in subtidal sandy sediments from the German Bight, *Flavobacteriia* were very abundant (Probandt *et al*., 2017). Furthermore, *Muricauda sp. MAR_2010_75* was isolated from the same region. The existence of a subset of denitrifiers which exclusively reduce N_2O to N_2 was shown recently for terrestrial soil metagenomes (Graf *et al*. 2014, Jones *et al*. 2012, Jones *et al*. 2014) and it has been hypothesized that these organisms could be important in mitigating N_2O releases from soils. The high abundances of a putative N_2O reducer along the North-West European coast suggest that permeable sandy sediments might enrich for organisms with this trait.

Sandy sediments – N_2O sink or source?

A previous study suggested that the intertidal sediments of the Wadden Sea were not a source of N_2O to the atmosphere (Kieskamp *et al*. 1991). However, Kieskamp *et al.,* (1991) did not take into account the permeable, advection driven nature of sandy sediments which has been shown to lead to severe underestimations of fluxes (Cook *et al*. 2006, de Beer *et al*. 2005, Gao *et al*. 2012). The evidence presented here indicates that the intertidal sandy sediments of the Wadden Sea are a source of N_2O. We demonstrated this experimentally by pumping water through a sediment core at velocities comparable to those measured in similar sediments *in situ,* finding that advective flow increases the flux of N_2O from the sediment to the overlying water. Furthermore, water column measurements made in the Wadden Sea revealed higher oversaturations of N_2O than have been observed so far in the nearby North Sea (Bange 2006, Law and Owens 1990). The significant enrichment of N_2O in water leaving the Wadden Sea region (as the tide recedes towards the German Bight) in comparison to water entering the region (Fig. 2) further indicates that the main source of N_2O is within the Wadden Sea. Similar tidal patterns are observed in the concentrations of NO_3^-, NO_2^- and NH_4^+ in the seawater and are attributed to activity and pore water advection within the tidal flat sediment (Grunwald *et al*., 2010). By combining

volumetric rates of N_2O consumption and production measured in March 2011 with modelled O_2 and NO_3^- and N_2O penetration depths we estimated that areal fluxes of N_2O out of the sediment are in the range of 0.11–1.51 μmol N-N_2O m^2 h^{-1}. This is in the same range as the air-sea fluxes determined from the *in situ* measurements of N_2O concentration in the water column above the sandflat in the same month (1.10 and 1.50 μmol N-N_2O m^{-2} h^{-1}).

A niche for N_2O reducing specialists

It is evident that the microbial community within the sediment denitrifies a large proportion of the NO_3^- that enters the Wadden Sea to N_2. In addition there is a production and emission of N_2O from the sediments, nevertheless, more than 98% of the N_2O produced is still reduced to N_2. The dominance of specialist N_2O reducing *Flavobacteriia* in the sediment, indicated by cell counts and metagenome/metatranscriptome *nosZ* reads, indicates that the *Flavobacteriia* likely consume a substantial proportion of the N_2O produced by other microorganisms (Fig. 5). N_2O respiration would offer the *Flavobacteriia* a niche within the sediment where they have little competition with other organisms. For example, competition for NO_3^- in this environment is likely to be intense, as there is both a high proportion of nitrate reducers (as seen in the molecular data) and an abundant, nitrate-accumulating microphytobenthos community (Marchant *et al*., 2014, Stief *et al*. 2013). N_2O respiration offers a thermodynamically favourable alternative to NO_3^- respiration, and moreover requires less investment in enzymes than expression of a full denitrification pathway, providing the *Flavobacteriia* with a niche for what seems to be a rather advantageous lifestyle.

Implications for N_2O emissions

Denitrification rates consistent with those measured in this study have been observed at different times and locations across the entire Wadden Sea (Gao *et al*. 2012, Marchant *et al*. 2014). In fact, denitrification rates have been shown to be generally high in permeable sandy sediments even in subtidal regions (Canion *et al*. 2014, Evrard *et al*., 2013, Gihring *et al*., 2010, Rao *et al.,* 2007, Sokoll *et al.,* 2016) and there is evidence to suggest that N_2O production rates are also high in subtidal sands (Marchant *et al.,* 2016). The consistency of these studies support a recent estimate that 60% of fixed N input from rivers and atmospheric deposition worldwide is denitrified within coastal sandy sediments (equating to 54 Tg) (Gao *et al*., 2012). Our areal fluxes indicate that 1 and 2% of this nitrate is denitrified incompletely to N_2O and released to the water column in the Wadden Sea. If this is the case in other regions, sandy coastal sediments may contribute substantially to N_2O emissions from the oceans, which are currently estimated to range between 5.4 Tg N yr^{-1} and 11 Tg N yr^{-1} (Bange 2008). Our combined results indicate that N_2O emissions from sands are tightly controlled by the network of N_2O-producing and N_2O-reducing microorganisms within the sediment.

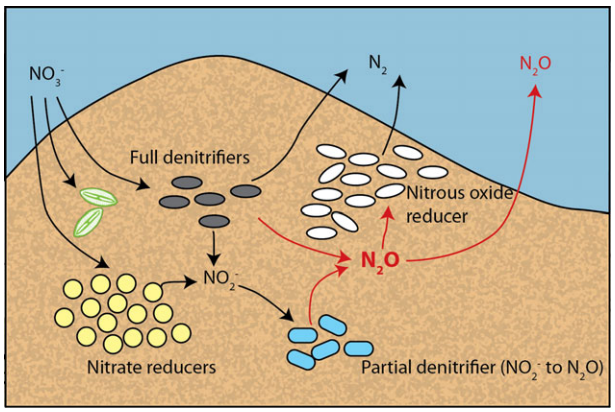

Fig. 5. Specialization of the denitrifying community in permeable sediments. Nitrate is advected into permeable sediments at rates orders of magnitude higher than diffusive fluxes. Nevertheless, competition for NO_3^- is intense, due to high nitrate reduction rates and uptake by diatoms. Intermediate production and release of N_2O by full denitrifiers is caused by rapid fluctuations in oxygen and nitrate availabilities due to changes in current velocity and sediment movement. Furthermore, partial denitrifiers which do not encode nitrous oxide reductase release N_2O into the sediment. The pool of N_2O provides an electron acceptor to specialized *Flavobacteriia*, however due to the movement of porewater, much of the N_2O is released to the water column before it is entirely consumed.

Experimental procedures

Study site and sampling

Sediment sampling was carried out at the Janssand sand flat (53.73515 ′N, 007.69913′E), which is located in the backbarrier region of the Wadden Sea, Germany. The flat consists of well sorted silicate sand, with a mean grain size of 176 μm and a porosity of 0.35 (upper 15 cm of sediment) (Billerbeck *et al*., 2006a, Billerbeck *et al.,* 2006b). The sand flat is inundated with seawater for around 10 h of each tidal cycle. When the tide is out, there is only a thin layer of water covering the sand flat. Previous studies have shown that oxygen can penetrate more than 5 cm while the tide is in, and while the tide is out only penetrates 1–2 cm (see Marchant *et al*., 2017, Jansen et al 2009).

Sediment was collected from the upper 5 cm of the sand flat and stored in washed plastic containers for transport before use in steady state core incubations, dynamic core incubations and microsensor experiments. Sediment for DNA analyses was immediately frozen at

−20°C, while sediment collected for RNA analyses was immersed in three volumes of RNA preservation solution (LifeGuardTM Soil Preservation Solution, MoBio), and stored at 4°C.

In situ N_2O concentrations

Sea water sampling to determine *in situ* N_2O concentrations was performed directly above the sand flat from a sampling platform on 21 March 2011. Over 12 h (beginning at low tide when the tide was rising and the flat was flooded with seawater until the flat was exposed again) samples were collected as technical triplicates from four water depths (5, 17, 47 and 80 cm above sediment surface) and averaged, leading to n = 14, 11, 6 and 3 respectively. Fewer samples were collected from 80 cm above the sediment surface as water only reached this height at three sampling points. Sampling was carried out using a lance and seawater was filled into 6 ml Exetainers (LabCo, UK) prefilled with 100 μl saturated $HgCl_2$ leaving no headspace. Sampling for *in situ* N_2O concentrations was also carried out from the main tidal inlet between the islands of Langeoog and Spiekeroog (53.44791 ′N, 007.418310′E) on 31 May 2011 using the ICBM ship 'Otzum', water was sampled from 3 m depth every 15 min over a 12 h period, using a niskin bottle and filled headspace free into 6 ml Exetainers (LabCo, UK) prefilled with 100 μl saturated $HgCl_2$ Tidal height data was provided by Thomas Badewien from the long term time series station at 53.450100'N, 007.401630'E.

Rate determinations

A number of experiments were carried out to investigate nitrification and denitrification rates within the sediment, these were comprised of isotope labelling experiments investigating nitrification rates, denitrification rates under steady state conditions, and denitrification rates under dynamic conditions. For all experiments sediment was gently homogenized and carefully filled into sediment cores (I.D. 10.3 cm, height 10 cm) ensuring no air bubbles were trapped. The cores were equipped with two way valves at both the top and bottom to allow the exchange of porewater within the core (Marchant *et al.,* 2014). Before measurements, cores were kept on a simulated tidal cycle consisting of repeated 6 h 'inundation' and 'exposure' periods. During 'inundation' seawater was supplied from the bottom of the core in cycles consisting of a 30 min period where water was pumped in at a rate of 2.5 ml min^{-1} followed by a 15 min period without pumping. (i.e. aerated seawater was pumped through for 6 h a day and no pumping occurred for 6 h).

Nitrification potential

Nitrification potential within the sediment was determined in triplicate sediment cores November 2011, April and July 2012 (parallel to denitrification measurements). The same incubation procedure was used as in Marchant *et al*., 2014, where the results from July 2012 are presented. Briefly, the entire porewater volume of the core was exchanged with aerated seawater which had been amended with $^{15}NH_4^+$ and $^{14}NO_2^-$. To achieve this 1 l of the amended water was pumped through the core from the bottom using a peristaltic pump. Porewater was then sampled passively from the bottom of the core into a 6 ml Exetainer (LabCo, UK) prefilled with 100 μl $HgCl_2$ saturated water. On average 12 time points were then taken over the next hour while oxygen was still detectable in the porewater. O_2, $^{15}NO_2^-$, $^{15}NO_3^-$ and $^{15}N{-}N_2O$ concentrations were determined as detailed below.

Denitrification under steady state anoxic conditions

Sediment incubations were carried out under 'steady state' anoxic conditions in August 2015. Briefly, sediment collected from the sand flat was kept on a simulated tidal cycle for 3 days and supplied with filtered North Sea water collected in March 2015 containing 20 μmol L^{-1} NO_3^-. On the third day, at the end of an 'exposure cycle' i.e. after the sediment had not received any water supply for 6 h, the sediment was carefully packed into three small flow through columns (height 10 cm, I.D. 3.7 cm). North Sea water (collected at the time of sampling, containing < 1 μmol L^{-1} NO_3) was deoxygenated by bubbling with He and amended with 60 μmol L^{-1} $^{15}NO_3^-$. Subsequently, it was pumped through the core at 1 ml min^{-1} until $^{15}N{-}N_2$ concentrations at the outlet were stable for more than 3 h (confirmed by online MIMS measurements). 3 × 12 ml porewater samples were collected passively from the outlet of each of the three cores in glass syringes and filled into 12 ml exetainers prefilled with 100 μl saturated $HgCl_2$. The ratios between the amount of produced NO_2^-, $^{15}N{-}N_2O$, $^{15}N{-}N_2$ were then determined as below.

Denitrification during changing conditions

Denitrification dynamics i.e. the production and consumption of NO_3^-, NO_2^-, N_2O and N_2 over time, were determined in sediment cores in March 2011. Three replicates cores were used, which were incubated with aerated $^{15}NO_3^-$ amended water using the method described above. The incubation was repeated on each core four times with 15, 50, 100 and 500 μM of added $^{15}NO_3^-$ respectively. After adding aerated, $^{15}NO_3^-$ labelled water to the core, on average 30 time points were collected

over the next 100–150 min, during this time the core became anoxic. At each time point, porewater was sampled passively from the bottom of the core into a 3 ml Exetainer (LabCo, UK) prefilled with 100 μl $HgCl_2$ saturated water. The same incubations were repeated subsequently in triplicate sediment cores in November 2011, April 2012 and July 2012, except 6 ml exetainers were used over 12 time points and only N_2 and N_2O production were determined (see Marchant *et al*., 2014 for N_2 production and DNRA rates from the same incubations).

Chemical and isotopic analysis

Nitrite and nitrate were determined using a chemiluminescence NO_x analyser after reduction to NO (Braman and Hendrix 1989). For gas analyses, a helium headspace was added to all exetainers after which they were equilibrated for at least 24 h. N_2O concentrations from *in situ* collected samples were determined on a gas chromatograph with a ^{63}Ni electron capture detector (Shimadzu GC-8A), calibration curves were determined from exetainers spiked with known concentrations of N_2O and partitioning of N_2O between the headspace and water was determined according to Weiss and Price (1980). For the denitrification rate determinations, $^{15}N—N_2$ and $^{15}N—N_2O$ production was determined by injecting gas from the headspace directly into a GC-IRMS (VG Optima, Manchester, UK). The isotope ratios of $^{28}N_2$, $^{29}N_2$ and $^{30}N_2$ and $^{44}N_2O$, $^{45}N_2O$ and $^{46}N_2O$ were determined respectively. The concentration of $^{29}N_2$ and $^{30}N_2$ were calculated from the excess of each relative to an air sample, as described in Holtappels *et al*., (2011), for N_2O 25 μl of N_2O was used as a standard (99.5%, Air Liquide, Germany). Rates were determined according to Nielsen (1992), using 'D_{tot}'. For nitrification rate determinations, $^{15}NO_3^-$ was converted to $^{15}N—N_2$ according to Füssel *et al.,* 2012, and measured as above. N_2O and N_2 in the steady state incubations were measured on an IsoPrime 100 IRMS coupled to a modified dual trapping tracegas module (Isoprime, Manchester, UK).

Areal fluxes across the sediment–water interface were determined from a transport model based on Elliott and Brooks (1997a, 1997b). The model simulates advective porewater flow in sands with rippled topography as a function of permeability, bedform geometry, and bottom water velocity. For reactive solutes (O_2, NO_3^-, N_2O), the model estimates the spatially averaged penetration depth, depending on the initial bottom water concentration and the reaction rate of the solute, assuming zero order kinetics. The same approach was used in Marchant *et al*., (2016) and Ahmerkamp *et al*. (2017), except for a modification made to calculate the N_2O flux out of the sediment (Supporting Information methods). For the transport terms in the model, observed ripple dimensions of 7 cm length and 2 cm height were applied. Permeability was set to 2.11×10^{-11} m^2 (determined from the measured median grain size of 176 μm using the empirical relationship from Gangi (1985) (see Ahmerkamp *et al*., 2017). Typical bottom water velocities observed over a tidal cycle were used ranging from 0.15 to 0.35 m s^{-1} (Gao *et al.,* 2012). For the reaction terms of the model bottom water concentrations of O_2 and NO_3^- were set to 265 μmol L^{-1} (air saturation at 13°C) and 32 μmol L^{-1} [average for the Wadden Sea, (Gao *et al*., 2012)], respectively. The reaction rates for O_2 respiration, denitrification and N_2O production/consumption were applied from the measurements made under dynamic conditions in March 2011 (see above).

The air-sea flux of N_2O was calculated from *in situ* measurements of water column N_2O concentrations, N_2O solubility and average wind speed using two different parameterizations according to Wanninkhof *et al*. (2009) and McGillis *et al*. (2001) (Supporting Information methods).

Microsensor incubations

In March 2010, the effect of porewater flow on N_2O and O_2 concentrations within the sediment and water overlying the sediment was investigated using microsensors. Porewater flow was changed in order to investigate whether this led to more N_2O transport to the overlying water. Sediment was filled into a core covered by a 5 cm lense of seawater (I.D. 5.4, sediment height 10 cm, total height 15 cm). The column was allowed to become anoxic, after which aerated seawater (amended with 500 μM NO_3-) was pumped from the bottom of the core at varying fluid flow velocities (11 cm h^{-1} and 21 cm h^{-1}). O_2 and N_2O microsensors were used to monitor concentrations at the surface of the sediment on top of the core. That is, once the fluid front had passed through the entire sediment core, repeated porewater profiles in the top 22 mm of the sediment and water column were carried out with N_2O and O_2 microsensors, constructed and calibrated as previously described (Andersen *et al*., 2001, Revsbech 1989, Schreiber *et al*. 2009).

Metagenomics

Two types of metagenomics were carried out on different samples, the first using a 454 GS FLX Titanium platform (500 bp) (Roche Applied Science), and the second using a HiSeq2000 Illumina platform (2 × 150 bp paired end reads) (San Diego, CA, USA).

Sediment samples for 454-based metagenomics were taken in October 2009 from 0–5 cm depth, and in March 2010 from 0-2 cm depth, a detailed description of the samples is given in Marchant *et al*., (2017). Briefly, three samples were taken in March, two of which were pooled and divided again into two technical replicates, named MarA

and MarB, the third sample (the biological replicate) is referred to as MarC. Samples Oct09 and MarA were sequenced in the same run and sample MarB was sequenced together with sample MarC. The four sequence data sets were submitted to the sequence read archive (http://trace.ncbi.nlm.nih.gov/Traces/sra/) under the Bioproject PRJNA174601 (Accession: SRP015924). The sample accession numbers are SRS365699, SRS365698, SRS365700 and SRS365701. A sample for Illumina metagenome sequencing was taken from the upper layer of the sand flat in April 2013, see Dyksma *et al*., (2018) for further details.

Metagenomic data analysis

The sequence data sets were pre-processed by removing identical reads via a CD-hit based algorithm (Li and Godzik 2006, Niu *et al*. 2010).

Taxonomy analysis – For taxonomy analysis, a reference database was generated by selecting a sequence subset of universally distributed protein orthologs from the FIGfam data base (Meyer *et al*. 2009) (ftp://ftp.theseed.org/FIGfams/ Release 12), see Supporting Information methods. The resulting sequence collection contained 65 001 sequences. A blastx search (E-value cutoff $1e^{-10}$) with the metagenomic reads against the generated protein orthologues database was performed, and the reads with a hit were assigned to the respective taxonomic class of the top hit FIGfam sequence (for more details see Supporting Information methods).

Functional gene detection

The 454 data were analysed using two different approaches to both detect and taxonomically assign functional denitrification genes within the metagenomes (*narG, napA, nirK, nirS*, *norB* and *nosZ).* In the first approach, Hidden Markov Models (HMM) were used to detect sequences encoding for functional genes, which were subsequently manually validated. The second approach utilized ROCker (Orellana *et al*., 2017), which detects sequences in short-read metagenomic data sets by modelling sliding-window bitscores. Reads encoding functional genes were taxonomically assigned using either MEGAN or Kaiju (Huson *et al*., 2011; Menzel *et al*. 2016). As these approaches gave similar results (Supporting Information Fig. S1), ROCker + Kaiju were used to analyse the Illumina dataset as the number of sequences precluded manual validation.

HMM-approach

For the detection of functional genes (*narG, napA, nirK, nirS*, *norB* and *nosZ)*, protein-coding genes were predicted in the metagenomic sequences and subsequently translated into correct protein sequences using PRODIGAL running in anonymous mode (Hyatt *et al*. 2010. The HMMsearch function of HMMer software package was used to identify reads of interest in the metagenomes (Eddy 2011). A collection of selected protein sequences (17–30 sequences per collection downloaded from UniProtKB, http://www.uniprot.org/ and Fungene http://fungene.cme.msu.edu/) were used to create profile HMM's. For *nirK*, additional sequences were used from Decleyre *et al.,* 2016.

An automated validation procedure of the reads was carried out against a gene validation database (see Supporting Information methods for further details), followed by manual validation. Sequencing coverage per base of a functional gene was calculated as follows: From the reads validated for each gene, first, the sum was calculated of all read bases aligning to a known functional gene (database sequence). Second, of all gene sequences in the database to which a read (partially) aligned, the average gene length was calculated. To obtain gene coverage per base values, the sum of the aligned read bases was divided by the calculated average gene length. An average coverage per base was calculated for the technical replicates (MarA and MarB).

Taxonomic assignment of functional denitrification genes – To investigate the phylogenetic affiliations of the validated *narG, napA, nirK, nirS*, *norB* and *nosZ* a blastp search (Altschul *et al.,* 1990) was run with default parameters against the NCBI nr database (November, 2015) using the translated and validated reads as query. Phylogenetic affiliations were assigned from the blastp search using LCA algorithm in MEGAN. A second approach utilized Kaiju (Menzel *et al*., 2016) using the nucleotide sequences (using the standard settings on the webserver: Reference database NCBI nr + euks, seg filter: on, runmode: greedy, minimum match length: 11, minimum match score: 75, allowed mistmatches: 5). For the generation of a phylogenetic tree, *narG, napA, nirK, nirS*, *norB* and *nosZ* genes for known taxa were chosen if they were among the top 10 blast hits of a read, and if the e-value was ≤0.0005. Otherwise the top hit sequence (clone/unknown taxon) was selected. The selected reference sequences for the phylogenetic trees were aligned with ClustalO and consensus trees were generated from 100 maximum likelihood trees generated using PhyML (Guindon *et al.,* 2010, Sievers *et al.,* 2011). The trees were visualized using the iTOL (Letunic and Bork 2016).

Identification of nirK functional genes in the 454 dataset

Of the 141 reads that passed the initial validation step for *nirK* identification, only 14 had a top 10 blastp hit that was similar to a sequence annotated as *nirK.* The

remaining hits were generally hypothetical proteins, or putative copper oxidases. To gain further insight into the identity of these sequences, the sequences from the metagenome were aligned against a reference library of *nirK* sequences. If they aligned at Asp62 and His237 (Decleyre *et al.,* 2016) they were validated. For those sequences which did not cover these regions of the reference sequences, then the nearest relative retrieved via a blastp search was aligned to the reference library instead. Only one further sequence was validated during this step. Four out of the 15 reads could not be assigned any taxonomic affiliation.

ROCker-approach

ROCker models were built specifically for either the 454 metagenomes (using a 500 bp average length for the in silico metagenome construction) or the Illumina metagenome (150 bp average length). Models were built for each functional gene using a collection of curated protein sequences and in the case of *napA*, *narG* and *norB* closely related outgroup protein sequences (downloaded from http://enve-omics.ce.gatech.edu/rocker/models and UniProtKB), according to Orellana *et al*., 2017. Sequences were then taxonomically assigned with MEGAN and Kaiju (454 datasets) or just Kaiju (Illumina dataset) and coverage per base calculated as before.

Odds ratio analysis

For each dataset an odds ratio analysis was carried out to determine whether *nosZ* was distributed evenly within the *Flavobacteriia* when compared to all denitrification reads within the *Gammaproteobacteria.* Briefly, the number of *Flavobacteriia nosZ* reads was first divided by the number of all other denitrifying reads in the *Flavobacteriia*, this number was then divided by the number of *Gammaproteobacteria nosZ* reads over the number of all other denitrifying reads in the *Gammaproteobacteria.*

Tidal cycle transcriptomics

Sediment sampling for transcriptomics was carried out on March 21 2011as detailed in Marchant *et al*., 2017. Six metatranscriptome libraries were generated from sediment sampled at six time points over a complete tidal cycle, each of these had between 1.2 and 8 million mRNA sequence reads with a mean length of 180 bp (Supporting Information Table S1). The sample accession numbers are SRS417277, SRS417279, SRS417280, SRS417281, SRS417282 and SRS417283.

Transcriptomic data analysis

The sequence data sets were pre-processed by Casava v1.8.4, and quality trimmed using Trimmomatic (Bolger *et al.,* 2014). SortMeRNA v2.0 (Kopylova *et al.,* 2012) was used to filter out rRNA reads. From the resulting non-rRNA reads identical reads were removed using CD-hit (Li and Godzik 2006) and translated into protein sequences using PRODIGAL (Hyatt *et al.,* 2010). The same HMM-approach detailed above was used identify transcripts within the sequence data. Taxonomic identities of transcripts were inferred using MEGAN (Huson *et al.,* 2011). In order to compare the distribution and abundance of Bacteroidetes functional gene transcripts over the tidal cycle, transcript abundances are calculated as read count per gene per kilobase of gene length and then normalized relative to the number of mRNA sequences in the respective metatranscriptome.

Acknowledgements

We thank the captains of the Doris von Ochtum and the Otzum. P. Stief for assistance with GC measurements and E. Robertson and L. Messer for assistance with field work. Ines Kattelmann and Rafael Szczepanowski assisted with DNA and RNA sequencing. This work was financially supported by the Max Planck Society, the ERC Starting Grant MASEM (to M.S.), and a Grant from the Federal State of North Rhine-Westphalia (to H.E.T.). The authors have no conflict of interest to declare.

References

Ahmerkamp, S., Winter, C., Janssen, F., Kuypers, M. M. M., and Holtappels, M. (2015) The impact of bedform migration on benthic oxygen fluxes. *J Geophys Res Biogeo* **120**: 2229–2242.

Ahmerkamp, S., Winter, C., Krämer, K., Beer, D.d., Janssen, F., Friedrich, J., *et al*. (2017) Regulation of benthic oxygen fluxes in permeable sediments of the coastal ocean. *Limnol Oceanogr* **62**: 1935–1954.

Altschul, S., Gish, W., Miller, W., Myers, E., and Lipman, D. (1990) Basic local alignment search tool. *J Mol Biol* **215**: 403–410.

Andersen, K., Kjaer, T., and Revsbech, N. P. (2001) An oxygen insensitive microsensor for nitrous oxide. *Sensors Actuators B-Cheml* **81**: 42–48.

Bakken, L. R., Bergaust, L., Liu, B., and Frostegård, Å. (2012) Regulation of denitrification at the cellular level: a clue to the understanding of N_2O emissions from soils. *Phil Trans Royal Soc B Biol Sci* **367**: 1226–1234.

Bange, H. W. (2006) Nitrous oxide and methane in European coastal waters. *Estuar Coast Shelf Sci* **70**: 361–374.

Bange, H. W. (2008)Gaseous nitrogen compounds (NO, N2O, N2, NH3) in the ocean . In *Nitrogen in the Marine Environment (2nd Edition)*. San Diego: Academic Press, pp. 51–94.

Bergaust, L., Shapleigh, J., Frostegard, A., and Bakken, L. (2008) Transcription and activities of NOx reductases in *Agrobacterium tumefaciens*: the influence of nitrate, nitrite and oxygen availability. *Environ Microbiol* **10**: 3070–3081.

Billerbeck, M., Werner, U., Bosselmann, K., Walpersdorf, E., and Huettel, M. (2006a) Nutrient release from an exposed intertidal sand flat. *Mar Ecol-Prog Ser* **316**: 35–51.

Billerbeck, M., Werner, U., Polerecky, L., Walpersdorf, E., de Beer, D., and Huettel, M. (2006b) Surficial and deep pore water circulation governs spatial and temporal scales of nutrient recycling in intertidal sand flat sediment. *Mar Ecol-Prog Ser* **326**: 61–76.

Bolger, A. M., Lohse, M., and Usadel, B. (2014) Trimmomatic: a flexible trimmer for Illumina sequence data. *Bioinformatics* **30**: 2114–2120.

Canion, A., Kostka, J., Gihring, T., Huettel, M., van Beusekom, J., Gao, H., *et al*. (2014) Temperature response of denitrification and anammox reveals the adaptation of microbial communities to in situ temperatures in permeable marine sediments that span 50° in latitude. *Biogeosciences* **11**: 309–320.

Cook, P. L. M., Wenzhofer, F., Rysgaard, S., Galaktionov, O. S., Meysman, F. J. R., Eyre, B. D., *et al*. (2006) Quantification of denitrification in permeable sediments: insights from a two-dimensional simulation analysis and experimental data. *Limnol Oceanogra-Meth* **4**: 294–307.

de Beer, D., Wenzhofer, F., Ferdelman, T. G., Boehme, S. E., Huettel, M., van Beusekom, J. E. E., *et al*. (2005) Transport and mineralization rates in North Sea sandy intertidal sediments, Sylt-Romo Basin, Wadden Sea. *Limnol Oceanogr* **50**: 113–127.

Decleyre, H., Heylen, K., Tytgat, B., and Willems, A. (2016) Highly diverse nirK genes comprise two major clades that harbour ammonium-producing denitrifiers. *BMC Genomics* **17**: 1–13.

Dendooven, L., and Anderson, J. M. (1994) Dynamics of reduction enzymes involved in the denitrification process in pasture soil. *Soil Biol Biochem* **26**: 1501–1506.

Dentener, F., Drevet, J., Lamarque, J. F., Bey, I., Eickhout, B., Fiore, A. M., *et al*. (2006) Nitrogen and sulfur deposition on regional and global scales: a multimodel evaluation. *Glob Biogeochem Cycles* **20**: GB4003. https://doi.org/10.1029/2005GB002672.

Dyksma, S., Bischof, K., Fuchs, B. M., Hoffmann, K., Meier, D., Meyerdierks, A., *et al*. (2016) Ubiquitous Gammaproteobacteria dominate dark carbon fixation in coastal sediments. *ISME J* **10**: 1939–1953.

Dyksma, S., Pjevac, P., Ovanesov, K., and Mussmann, M. (2018) Evidence for H_2 consumption by uncultured *Desulfobacterales* in coastal sediments. *Environ Microbiol* **20**: 450–461. https://doi.org/10.1111/1462-2920.13880.

Eddy, S. R. (2011) Accelerated profile HMM searches. *PLoS Comput Biol* **7**: e1002195.

Elliott, A. H., and Brooks, N. H. (1997a) Transfer of nonsorbing solutes to a streambed with bed forms; theory. *Water Resour Res* **33**: 123–136.

Elliott, A. H., and Brooks, N. H. (1997b) Transfer of nonsorbing solutes to a streambed with bed forms: laboratory experiments. *Water Resour Res* **33**: 137–151.

Emery, K. O. (1968) Relict sediments on continental shelves of world. *AAPG Bull* **52**: 445–464.

Evrard, V., Glud, R. N., and Cook, P. L. (2013) The kinetics of denitrification in permeable sediments. *Biogeochemistry* **113**: 563–572.

Foster, S. Q., and Fulweiler, R. W. (2016) Sediment nitrous oxide fluxes are dominated by uptake in a temperate estuary. *Front Mar Sci* **3**. https://doi.org/10.3389/fmars.2016.00040

Füssel, J., Lam, P., Lavik, G., Jensen, M. M., Holtappels, M., Gunter, M., *et al*. (2012) Nitrite oxidation in the Namibian oxygen minimum zone. *ISME J* **6**: 1200–1209.

Ganesh, S., Bristow, L. A., Larsen, M., Sarode, N., Thamdrup, B., and Stewart, F. J. (2015) Size-fraction partitioning of community gene transcription and nitrogen metabolism in a marine oxygen minimum zone. *ISME J* **9**: 2682–2696.

Gangi, A. F. (1985) Permeability of unconsolidated sands and porous rocks. *J Geophys Res Solid Earth* **90**: 3099–3104.

Gao, H., Schreiber, F., Collins, G., Jensen, M. M., Kostka, J. E., Lavik, G., *et al*. (2010) Aerobic denitrification in permeable Wadden Sea sediments. *ISME J* **4**: 417–426.

Gao, H., Matyka, M., Liu, B., Khalili, A., Kostka, J. E., Collins, G., *et al*. (2012) Intensive and extensive nitrogen loss from intertidal permeable sediments of the Wadden Sea. *Limnol Oceanogr* **57**: 185–198.

Gihring, T. M., Canion, A., Riggs, A., Huettel, M., and Kostka, J. E. (2010) Denitrification in shallow, sublittoral Gulf of Mexico permeable sediments. *Limnol Oceanogr* **55**: 43–54.

Graf, D. R. H., Jones, C. M., and Hallin, S. (2014) Intergenomic comparisons highlight modularity of the denitrification pathway and underpin the importance of community structure for N2O emissions. *PLoS One* **9**. https://doi.org/10.1371/journal.pone.0114118.

Gruber, N., and Galloway, J. N. (2008) An earth-system perspective of the global nitrogen cycle. *Nature* **451**: 293–296.

Grunwald, M., Dellwig, O., Kohlmeier, C., Kowalski, N., Beck, M., Badewien, T. H., *et al*. (2010) Nutrient dynamics in a back barrier tidal basin of the southern North Sea: time-series, model simulations, and budget estimates. *J Sea Res* **64**: 199–212.

Guindon, S., Dufayard, J. F., Lefort, V., Anisimova, M., Hordijk, W., and Gascuel, O. (2010) New algorithms and methods to estimate maximum-likelihood phylogenies: assessing the performance of Phy ML 3.0. *Syst Biol* **59**: 307–321.

Hall, S. J. (2002) The continental shelf benthic ecosystem: current status, agents for change and future prospects. *Environ Conserv* **29**: 350–374.

Hallin, S., Philippot, L., Löffler, F. E., Sanford, R. A., and Jones, C. M. (2018) Genomics and ecology of novel N_2O-reducing microorganisms. *Trends Microbiol* **26**: 43–55.

Henry, S., Bru, D., Stres, B., Hallet, S., and Philippot, L. (2006) Quantitative detection of the nos Z gene, encoding nitrous oxide reductase, and comparison of the abundances of 16S rRNA, nar G, nirK, and nos Z genes in soils. *Appl Environ Microbiol* **72**: 5181–5189.

Holtappels, M., Lavik, G., Jensen, M. M., and Kuypers, M. M. M. (2011) ^{15}N-labeling experiments to dissect the contributions of heterotrophic denitrification and anammox to nitrogen removal in the OMZ waters of the ocean . In *Methods in Enzymology*, Klotz, M. G. (ed), pp. 223–251. Elsevier Academic Press, New York.

Huettel, M., Roy, H., Precht, E., and Ehrenhauss, S. (2003) Hydrodynamical impact on biogeochemical processes in aquatic sediments. *Hydrobiologia* **494**: 231–236.

Huettel, M., Berg, P., and Kostka, J. E. (2014) Benthic exchange and biogeochemical cycling in permeable sediments. *Annu Rev Mar Sci* **6**: 23–51.

Huson, D. H., Mitra, S., Ruscheweyh, H.-J., Weber, N., and Schuster, S. C. (2011) Integrative analysis of environmental sequences using MEGAN4. *Genome Res* **21**: 1552–1560.

Hyatt, D., Chen, G.-L., LoCascio, P. F., Land, M. L., Larimer, F. W., and Hauser, L. J. (2010) Prodigal: prokaryotic gene recognition and translation initiation site identification. *BMC Bioinformatics* **11**: 1–11.

Jansen, S., Walpersdorf, E., Werner, U. et al. (2009) *Ocean Dynamics* **59**: 317. https://doi.org/10.1007/s10236-009-0179-4

Janssen, F., Huettel, M., and Witte, U. (2005) Pore-water advection and solute fluxes in permeable marine sediments (II): benthic respiration at three sandy sites with different permeabilities (German bight, North Sea). *Limnol Oceanogr* **50**: 779–792.

Jones, C. M., Stres, B., Rosenquist, M., and Hallin, S. (2008) Phylogenetic analysis of nitrite, nitric oxide, and nitrous oxide respiratory enzymes reveal a complex evolutionary history for denitrification. *Mol Biol Evol* **25**: 1955–1966.

Jones, C. M., Graf, D. R. H., Bru, D., Philippot, L., and Hallin, S. (2012) The unaccounted yet abundant nitrous oxide-reducing microbial community: a potential nitrous oxide sink. *ISME J* **7**: 417–426.

Jones, C. M., Spor, A., Brennan, F. P., Breuil, M.-C., Bru, D., and Lemanceau, P. (2014) Recently identified microbial guild mediates soil N_2O sink capacity. *Nat Clim Chang* **4**: 801–805.

Kalvelage, T., Lavik, G., Lam, P., Contreras, S., Arteaga, L., Loscher, C. R., *et al*. (2013) Nitrogen cycling driven by organic matter export in the South Pacific oxygen minimum zone. *Nat Geosci* **6**: 228–234.

Kieskamp, W. M., Lohse, L., Epping, E., and Helder, W. (1991) Seasonal-variation in denitrification rates and nitrous oxide fluxes in intertidal sediments of the western Wadden Sea. *Mar Ecol-Prog Ser* **72**: 145–151.

Kopylova, E., Noé, L., and Touzet, H. (2012) Sort MeRNA: fast and accurate filtering of ribosomal RNAs in metatranscriptomic data. *Bioinformatics* **28**: 3211–3217.

Kuypers, M. M., Marchant, H. K., and Kartal, B. (2018) The microbial nitrogen-cycling network. *Nat Rev Microbiol* **16**: 263.

Law, C. S., and Owens, N. J. P. (1990) Denitrification and nitrous oxide in the North Sea. *Neth J Sea Res* **25**: 65–74.

Letunic, I., and Bork, P. (2016) Interactive tree of life (iTOL) v3: an online tool for the display and annotation of phylogenetic and other trees. *Nucleic Acids Res* **44**: W242–W245.

Li, W., and Godzik, A. (2006) Cd-hit: a fast program for clustering and comparing large sets of protein or nucleotide sequences. *Bioinformatics* **22**: 1658–1659.

Lilja, E. E., and Johnson, D. R. (2016) Segregating metabolic processes into different microbial cells accelerates the consumption of inhibitory substrates. *ISME J* **10**: 1568–1578.

Marchant, H. K., Lavik, G., Holtappels, M., and Kuypers, M. M. M. (2014) The fate of nitrate in intertidal permeable sediments. *PLoS One* **9**: e104517.

Marchant, H. K., Holtappels, M., Lavik, G., Ahmerkamp, S., Winter, C., and Kuypers, M. M. M. (2016) Coupled nitrification–denitrification leads to extensive N loss in subtidal permeable sediments. *Limnol Oceanogr* **61**: 1033–1048.

Marchant, H. K., Ahmerkamp, S., Lavik, G., Tegetmeyer, H. E., Graf, J., Klatt, J. M., Holtappels, M., Walpersdorf, E. and Kuypers, M. M. (2017). Denitrifying community in coastal sediments performs aerobic and anaerobic respiration simultaneously. *The ISME journal* **11**: 1799–1812.

McGillis, W. R., Edson, J. B., Ware, J. D., Dacey, J. W. H., Hare, J. E., Fairall, C. W., *et al*. (2001) Carbon dioxide flux techniques performed during GasEx-98. *Mar Chem* **75**: 267–280.

Menzel, P., Ng, K. L., and Krogh, A. (2016) Fast and sensitive taxonomic classification for metagenomics with Kaiju. *Nat Commun* **7**: 11257.

Meyer, R. L., Allen, D. E., and Schmidt, S. (2008) Nitrification and denitrification as sources of sediment nitrous oxide production: a microsensor approach. *Mar Chem* **110**: 68–76.

Meyer, F., Overbeek, R., and Rodriguez, A. (2009) FIGfams: yet another set of protein families. *Nucleic Acids Res* **37**: 6643–6654.

Murray, R. H., Erler, D. V., and Eyre, B. D. (2015) Nitrous oxide fluxes in estuarine environments: response to global change. *Glob Chang Biol* **21**: 3219–3245.

Musat, N., Werner, U., Knittel, K., Kolb, S., Dodenhof, T., van Beusekom, J. E. E., *et al*. (2006) Microbial community structure of sandy intertidal sediments in the North Sea, Sylt-Romo Basin, Wadden Sea. *Syst Appl Microbiol* **29**: 333–348.

Mussmann, M., Pjevac, P., Krüger, K., and Dyksma, S. (2017) Genomic repertoire of the Woeseiaceae/JTB255, cosmopolitan and abundant core members of microbial communities in marine sediments. *ISME J* **11**: 1276.

Naqvi, S. W. A., Jayakumar, D. A., Narvekar, P. V., Naik, H., Sarma, V. V. S. S., D'Souza, W., *et al*. (2000) Increased marine production of N_2O due to intensifying anoxia on the Indian continental shelf. *Nature* **408**: 346–349.

Nielsen, L. P. (1992) Denitrification in sediment determined from nitrogen isotope pairing. *FEMS Microbiol Ecol* **86**: 357–362.

Niu, B., Fu, L., Sun, S., and Li, W. (2010) Artificial and natural duplicates in pyrosequencing reads of metagenomic data. *BMC Bioinformatics* **11**: 187.

Orellana, L. H., Rodriguez, L. M., Konstantinos, R., and Konstantinidis, T. (2017) ROCker: accurate detection and quantification of target genes in short-read metagenomic data sets by modeling sliding-window bitscores. *Nucleic Acids Res* **45**: e14. https://doi.org/10.1093/nar/gkw900.

Otte, S., Grobben, N. G., Robertson, L. A., Jetten, M. S., and Kuenen, J. G. (1996) Nitrous oxide production by *Alcaligenes faecalis* under transient and dynamic aerobic and anaerobic conditions. *Appl Environ Microbiol* **62**: 2421–2426.

Philippot, L., Mirleau, P., Mazurier, S., Siblot, S., Hartmann, A., Lemanceau, P., *et al*. (2001) Characterization and transcriptional analysis of *Pseudomonas fluorescens* denitrifying clusters containing the nar, nir, nor and nos genes. *Biochim Biophys Acta* **1517**: 436–440.

Philippot, L., and Hallin, S. (2005) Finding the missing link between diversity and activity using denitrifying bacteria

as a model functional community. *Curr Opin Microbiol* **8**: 234–239.

Philippot, L., Spor, A., Hénault, C., Bru, D., Bizouard, F., Jones, C. M., *et al*. (2013) Loss in microbial diversity affects nitrogen cycling in soil. *ISME J* **7**: 1609–1619.

Precht, E., and Huettel, M. (2004) Rapid wave-driven advective pore water exchange in a permeable coastal sediment. *J Sea Res* **51**: 93–107.

Probandt, D., Knittel, K., Tegetmeyer, H. E., Ahmerkam, S., Holtappels, M., and Amann, R. (2017) Permeability shapes bacterial communities in sublittoral surface sediments. *Environ Microbiol* **19**: 1584–1599. https://doi.org/10.1111/1462-2920.13676.

Rao, A. M. F., McCarthy, M. J., Gardner, W. S., and Jahnke, R. A. (2007) Respiration and denitrification in permeable continental shelf deposits on the South Atlantic bight: rates of carbon and nitrogen cycling from sediment column experiments. *Cont Shelf Res* **27**: 1801–1819.

Ravishankara, A. R., Daniel, J. S., and Portmann, R. W. (2009) Nitrous oxide (N_2O): the dominant ozone-depleting substance emitted in the 21st century. *Science* **326**: 123–125.

Revsbech, N. P. (1989) An oxygen microsensor with a guard cathode. *Limnol Oceanogr* **34**: 474–478.

Rizvi S (2014). Ecology and cultivation of unknown Flavobacteria in tidal sediments. Master thesis. Witzenhausen: University of Kassel.

Roco, C. A., Bergaust, L. L., Bakken, L. R., Yavitt, J. B., and Shapleigh, J. P. (2016) Modularity of nitrogen-oxide reducing soil bacteria: linking phenotype to genotype. *Environ Microbiol* **19**: 2507–2519.

Sanford, R. A., Wagner, D. D., Wu, Q., Chee-Sanford, J. C., Thomas, S. H., and Cruz-Garcia, C. (2012) Unexpected nondenitrifier nitrous oxide reductase gene diversity and abundance in soils. *Proc Natl Acad Sci U S A* **109**: 19709–19714.

Schreiber, F., Loeffler, B., Polerecky, L., Kuypers, M. M. M., and de Beer, D. (2009) Mechanisms of transient nitric oxide and nitrous oxide production in a complex biofilm. *ISME J* **3**: 1301–1313.

Schreiber, F., Wunderlin, P., Udert, K. M., and Wells, G. F. (2012) Nitric oxide and nitrous oxide turnover in natural and engineered microbial communities: biological pathways, chemical reactions and novel technologies. *Front Microbiol* **3**: 1–24. https://doi.org/10.3389/fmicb.2012.00372.

Schutte, C. A., Joye, S. B., Wilson, A. M., Evans, T., Moore, W. S., and Casciotti, K. (2015) Intense nitrogen cycling in permeable intertidal sediment revealed by a nitrous oxide hot spot. *Glob Biogeochem Cycles* **29**: 1584–1598.

Seitzinger, S. P., Pilson, M. E. Q., and Nixon, S. W. (1983) Nitrous oxide production in nearshore marine sediments. *Science* **222**: 1244–1246.

Seitzinger, S. P., Kroeze, C., and Styles, R. V. (2000) Global distribution of N_2O emissions from aquatic systems: natural emissions and anthropogenic effects. *Chemosph-Glob Change Sci* **2**: 267–279.

Shapleigh, J. (2007)The denitrifying bacteria . In *The Prokaryotes: A Handbook on the Biology of Bacteria*, Dworkin, M. (ed). New York, NY: Springer-Verlag, pp. 769–792.

Sievers, F., Wilm, A., Dineen, D., Gibson, T. J., Karplus, K., Li, W., *et al*. (2011) Fast, scalable generation of high-quality protein multiple sequence alignments using Clustal omega. *Mol Syst Biol* **7**: 539.

Šimek, M., and Cooper, J. E. (2002) The influence of soil pH on denitrification: progress towards the understanding of this interaction over the last 50 years. *Eur J Soil Sci* **53**: 345–354.

Simon, J., and Klotz, M. G. (2013) Diversity and evolution of bioenergetic systems involved in microbial nitrogen compound transformations. *Biochim Biophys Acta* **1827**: 114–135.

Sokoll, S., Lavik, G., Sommer, S., Goldhammer, T., Kuypers, M. M. M., and Holtappels, M. (2016) Extensive nitrogen loss from permeable sediments off North-West Africa. *J Geophys Res Biogeo* **121**: 1144–1157.

Stief, P., Kamp, A., and de Beer, D. (2013) Role of diatoms in the spatial-temporal distribution of intracellular nitrate in intertidal sediment. *PLoS One* **8**: e73257–e73257.

Usui, T., Koike, I., and Ogura, N. (2001) N_2O production, nitrification and denitrification in an estuarine sediment. *Estuar Coast Shelf Sci* **52**: 769–781.

van Beusekom, J. E. E. (2005) A historic perspective on Wadden Sea eutrophication. *Helgol Mar Res* **59**: 45–54.

Wanninkhof, R., Asher, W. E., Ho, D. T., Sweeney, C., and McGillis, W. R. (2009) Advances in quantifying Air-Sea gas exchange and environmental forcing. *Annu Rev Mar Sci* **1**: 213–244.

Weiss, R. F., and Price, B. A. (1980) Nitrous oxide solubility in water and seawater. *Mar Chem* **8**: 347–359.

Wood, D. W., Setubal, J. C., Kaul, R., Monks, D. E., Kitajima, J. P., Okura, V. K., *et al*. (2001) The genome of the natural genetic engineer *Agrobacterium tumefaciens* C58. *Science* **294**: 2317–2323.

Supporting Information

Additional Supporting Information may be found in the online version of this article at the publisher's web-site:

Table S1. Read numbers and statistics of metatranscriptomes. The two values for each transcriptome represent lanes 1 and 2 of the Sequencing flowcell.

Table S2. Taxonomic distribution of Wadden Sea sediment metagenomes in percent. * Indicates that the value is more than 1SD different from the mean. Samples taken in March all showed similar distributions, for example Bacillariophyta were most common followed by Streptophyta, Chordata, Proteobacteria, Bacteroides, Ascomyta/Athropoda and Planctomycetes. October showed the same pattern, except Bacilliariophyta were much less common (highlighted in bold), as a result all other percentages were higher, nevertheless they fell within 1.5 SD of the mean. All sequence reads were submitted to a blastx search against a reference database that was set up from selected FIGfam sequences of widely distributed gene orthologs, to ensure evenly distributed numbers of sequences per taxon. MarA and MarB are metagenomes from two DNA extracts of the same (homogenized) sediment sample

Table S3. Distribution of functional denitrification genes among the Gammproteobacteria in the sediment. Data is shown in gene coverage per base, which refers to the sum of bases in the analysed metagenomes that aligned to the functional gene of interest divided by the average length of that functional gene. Assignments using both MEGAN and

Kauji are shown for comparison from the 454 data from the HMM-based approach. For the ROCker based approach data is shown from the 454 dataset and the more deeply sequenced illumina dataset, note that the number of Gammaproteobacteria that could not be classified further is higher in the illumina data due to the shorter readlength.

Fig. S1. Comparison of different sequencing technologies, methods to identify functional genes and methods to taxonomically classify reads. Panel a) and b) are the same as in Fig. in the main text. Panel c) and d) show a comparison of the 454 dataset using Hidden Markov Models to detect functional genes and either Kaiju (c) or MEGAN (d) for taxonomic classification. The more common HMM-approach required lengthy manual post validation before the final identification of 780 reads. This was not feasible for the Illumina dataset (in total 34043 reads were identified as napA, narG, nirS, nirK, norB or nosZ).

Fig. S2. Comparison of 454 metagenome functional nosZ gene assignments at the genus level using MEGAN (a) or Kaiju (b), and of the Illumina reads using Kaiju. Further Flavobacterial genus could be identified in the Illumina metagenome than the 454 metagenomes, but all had a coverage per base of less than 1 and are note shown. Note that the shorter sequence length in the illumina metagenome means that less reads can be assigned at this level. Kaiju output is from the webserver with the standard settings: Reference database NCBI nr + euks, seg filter: on, runmode: greedy, minimum match length: 11, minimum match score: 75, allowed mistmatches: 5)

Fig. S3. a) Relative transcript abundance of all identified denitrification functional genes over a tidal cycle, using phylogenetic assignments from MEGAN. Relative transcript abundance refers to the read count per gene per kilobase of gene length and divided by the total mRNA reads in each respective metatranscriptome. b and c) comparison of nosZ assignments using either MEGAN or Kaiju

Fig. S4. Relative transcript abundance of Flavobacteria functional genes over a tidal cycle. Relative transcript abundance refers to the read count per gene per kilobase of gene length and divided by the total mRNA reads in each respective metatranscriptome. No nirS reads were detected.

Fig. S5. Taxonomic distribution of nosZ gene transcripts affiliated to the Flavobacteria over a tidal cycle, using Megan (a) or Kaiju (b). Kaiju output is from the webserver with the standard settings: Reference database NCBI nr + euks, seg filter: on, runmode: greedy, minimum match length: 11, minimum match score: 75, allowed mistmatches: 5

Fig. S6. Depth profiles of N_2O concentrations (left) and O_2 concentrations (right) within the sediment measured with microsensors under realistic flow velocities, N_2O concentrations in the overlying water between the profiles are shown in Fig. . of the main text. The initial profile was carried out while the core was anoxic and subsequent profiles took place while aerated seawater (amended with 500 μM NO_3-) was pumped upwards from the bottom of the core. Fluid velocity in the core was 11 cm h^{-1} during profile 1 and 2 and 21 cm h^{-1} in profile 3 and 4. Therefore each subsequent profile represents a condition in which nitrate supply and oxygen concentration in the upper core was increased. See Fig. 2 in the main Text for exact timing of sediment profiles.

Fig. S7. Phylogenetic tree of nirS relatives from validated metagenome sequences. Maximum likelihood tree (100 bootstraps) constructed of nirS database sequences which were the top blast hit of validated nirS reads within the metagenomes. Highlights show the phylogeny of the reference sequences and the number of reads hitting each reference sequence in each season is shown in the boxes. Highlighted in bold are the full and partial sequences of JTB255-MBG.

Fig. S8. Phylogenetic tree of nosZ relatives. Maximum likelihood tree (100 bootstraps) of nosZ database sequences which were the top blast hit of validated nosZ reads within the metagenomes. The cytochrome C oxidase gene of *Paracoccus denitrificans* is included as an outgroup. Highlights show the phylogeny of the reference sequences and the number of reads hitting each reference sequence in each season is shown in the boxes.